

Simulation of the clinical procedure by digital intraoral palpation of the greatest prominence of the Infrazygomatic crest for mini-implants insertion

Simulação do procedimento clínico por palpação digital intraoral da maior proeminência da crista Infrazigomática para inserção de mini-implantes

Simulación del procedimiento clínico por palpación digital intraoral de la mayor prominencia de la crista Infracigomática para inserción de mini-implantes

Received: 03/25/2022 | Reviewed: 04/03/2022 | Accept: 04/11/2022 | Published: 04/15/2022

Oscar Mario Antelo

ORCID: <https://orcid.org/0000-0001-8944-5329>
Pontifícia Universidade Católica do Paraná, Brazil
E-mail: oarortodoncia@hotmail.com

Armando Yukio Saga

ORCID: <https://orcid.org/0000-0002-4585-6588>
Pontifícia Universidade Católica do Paraná, Brazil
E-mail: saga.armando@gmail.com

Ariel Adriano Reyes

ORCID: <https://orcid.org/0000-0003-0699-8759>
Pontifícia Universidad Católica Madre y Maestra, Dominican Republic
E-mail: drarielreyes@gmail.com

Thiago Martins Meira

ORCID: <https://orcid.org/0000-0003-3862-5797>
Universidade do Estado da Bahia, Brazil
E-mail: thiagomartinsm@gmail.com

Sérgio Aparecido Ignácio

ORCID: <https://orcid.org/0000-0002-8242-3781>
Pontifícia Universidade Católica do Paraná, Brazil
E-mail: s.ignacio@pucpr.br

Orlando Motohiro Tanaka

ORCID: <https://orcid.org/0000-0002-1052-7872>
Pontifícia Universidade Católica do Paraná, Brazil
E-mail: tanakaom@gmail.com

Abstract

The objective of this cross-sectional retrospective study was to simulate using cone-beam computed tomography (CBCT) in adults, the clinical procedure performed by intraoral digital palpation of the greatest prominence (GP) of the Infrazygomatic crest (IZC) for mini-implants (MIs) insertion. CBCT images of 34 adults (14 men, 20 women), aged 18.0 to 57.7 years (mean, 32.2 years) were selected. On 3D reconstruction, the GP of the IZC region was determined using the anatomical morphology, and its anteroposterior position on the selected axial slice was evaluated relative to the dental reference located between the maxillary first and second molars (U6–U7). On the selected coronal slice, two reference lines were established to evaluate the insertion angle and insertion depth (IZC thickness) for MIs. The same procedure was performed on slices with intervals of 1 mm mesially as well as distally up to reach 4 mm. The right and left sides were measured. In relation to U6-U7, the GP of the IZC was 0.19 mm (± 1.79) mesial on the right side and 0.29 mm (± 1.65) mesial on the left side. The greatest bone thickness of the IZC was 4.95 mm (± 2.39) on the right side, 3.81 mm distal from U6-U7, and 4.79 mm (± 2.13) on the left side, 3.71 mm distal from U6-U7. The GP-IZC determined visually on the 3D reconstruction, did not present the greatest bone thickness. The bone tended to gradually become thicker distal to the GP-IZC and the dental reference U6-U7.

Keywords: Infrazygomatic crest; Mini-implants; Skeletal anchorage.

Resumo

O objetivo deste estudo transversal retrospectivo foi simular, por meio de tomografia computadorizada de feixe cônico (TCFC) em adultos, o procedimento clínico realizado por palpação digital intraoral da maior proeminência (MP) da crista Infrazigomática (CIZ) para inserção de mini-implantes (MIs). Foram selecionadas imagens de TCFC de 34 adultos (14 homens, 20 mulheres), com idades entre 18,0 e 57,7 anos (média de 32,2 anos). Na reconstrução 3D, a MP da região da CIZ foi determinada pela morfologia anatômica, e sua posição anteroposterior no corte axial selecionado foi avaliada em relação à referência dentária localizada entre os primeiros e segundos molares superiores (U6–U7). No corte coronal

selecionado, duas linhas de referência foram estabelecidas para avaliar o ângulo de inserção e a profundidade de inserção (espessura da CIZ) para MIs. O mesmo procedimento foi realizado em cortes com intervalos de 1 mm mesial e distalmente até atingir 4 mm. Os lados direito e esquerdo foram medidos usando os mesmos procedimentos. Em relação a U6-U7, a MP da região CIZ foi 0,19 mm ($\pm 1,79$) mesial do lado direito e 0,29 mm ($\pm 1,65$) mesial do lado esquerdo. A maior espessura óssea do CIZ foi de 4,95 mm ($\pm 2,39$) no lado direito, 3,81 mm distal de U6-U7 e 4,79 mm ($\pm 2,13$) no lado esquerdo, 3,71 mm distal de U6-U7. A MP-CIZ determinado visualmente na reconstrução 3D, não apresentou a maior espessura óssea. O osso tendeu a tornar-se, gradualmente, mais espesso distalmente ao MP-CIZ e à referência odontológica U6-U7.

Palavras-chave: Crista Infracigomática; Mini-implantes; Ancoragem esquelética.

Resumen

El objetivo de este estudio retrospectivo transversal fue simular mediante tomografía computarizada de haz cónico (TCHC) en adultos, el procedimiento clínico realizado por palpación digital intraoral de la mayor prominencia (MP) de la cresta Infracigomática (CIC) para la inserción de mini-implantes (MIs). Se seleccionaron imágenes CBCT de 34 adultos (14 hombres, 20 mujeres), de 18,0 a 57,7 años (media, 32,2 años). En la reconstrucción 3D, se determinó la MP de la CIC utilizando la morfología anatómica, y se evaluó su posición anteroposterior en el corte axial seleccionado en relación con la referencia dental ubicada entre los primeros y segundos molares maxilares (U6-U7). En el corte coronal seleccionado, se establecieron dos líneas de referencia para evaluar el ángulo de inserción y la profundidad de inserción (espesura CIC) para MIs. El mismo procedimiento se realizó en cortes con intervalos de 1 mm tanto mesialmente como distalmente hasta llegar a 4 mm. Los lados derecho e izquierdo se midieron utilizando los mismos procedimientos. En relación a U6-U7, la MP de la CIC fue de 0,19 mm ($\pm 1,79$) mesial del lado derecho y 0,29 mm ($\pm 1,65$) mesial del lado izquierdo. El mayor grosor óseo de la CIC fue de 4,95 mm ($\pm 2,39$) del lado derecho, 3,81 mm distal de U6-U7, y de 4,79 mm ($\pm 2,13$) del lado izquierdo, 3,71 mm distal de U6-U7. La MP-CIC determinada visualmente sobre la reconstrucción 3D, no presentó la mayor espesura ósea. El hueso tendía a volverse gradualmente más espeso distal a la MP-CIC y la referencia dental U6-U7.

Palabras clave: Cresta Infracigomática; Mini-implantes; Anclaje esquelético.

1. Introduction

Patients often reject extractions in orthodontic treatment and demand for alternative treatment to avoid them. (Keles & Sayinsu, 2000) Alternatively, perform distalization of maxillary molars is relatively difficult compared with other types of tooth movements. (Liou et al., 2004) Successful complete maxillary dentition distalization depends on consistent temporary skeletal anchorage with MIs, placed distant from the roots. (Ali et al., 2016; Lima Jr et al., 2022; Wu et al., 2011)

The IZC is one of the anatomical sites distant from roots, which allows unobstructed tooth movement during complete distalization of the maxillary dentition, decreasing the chance of root contact and damage. (Uribe et al., 2015; Vargas et al., 2020) The IZC is a pillar of cortical bone located in the lower part of the zygomatic process of the maxilla, intraorally, it is a bony protuberance palpable along the curvature between the alveolar process and the zygomatic process of the maxilla. (Liou et al., 2007) Anatomically, the IZC has two cortical plates: the buccal cortical plate and the cortical plate of the maxillary sinus floor. This anatomical advantage allows bicortical fixation, which contributes in improving the primary stability of the MI. (Jia et al., 2018)

According to Liou et al (Liou et al., 2007) and Baumgaertel et al (Baumgaertel & Hans, 2009) the IZC is located on the buccal surface of the zygomatic process of the maxilla, above the first permanent molars. According to De Clerck et al (De Clerck et al., 2002) and Chang et al (Chang et al., 2019) the IZC, located between the first and second molars, is the chosen site for placing MIs at a safe distance from the roots of maxillary molars.

Some studies have evaluated the IZC in terms of bone thickness, MI insertion angle and height using CBCT. (Baumgaertel & Hans, 2009; Lee et al., 2013; Liou et al., 2007; Murugesan & Sivakumar, 2020; Santos et al., 2017)

Due to the growing demand of adult patients seeking conservative orthodontic treatment avoiding extractions, and the frequent use of MIs as temporary skeletal anchorage, sometimes the clinician is based solely on his/her knowledge and clinical experience to insert MIs in the IZC region without CBCT of the area. For this reason, the aim of this study was to simulate using CBCT, the clinical maneuver, where the operator decides the insertion site of the MI by intraoral palpation of the greatest

prominence of the IZC in Adults.

2. Methodology

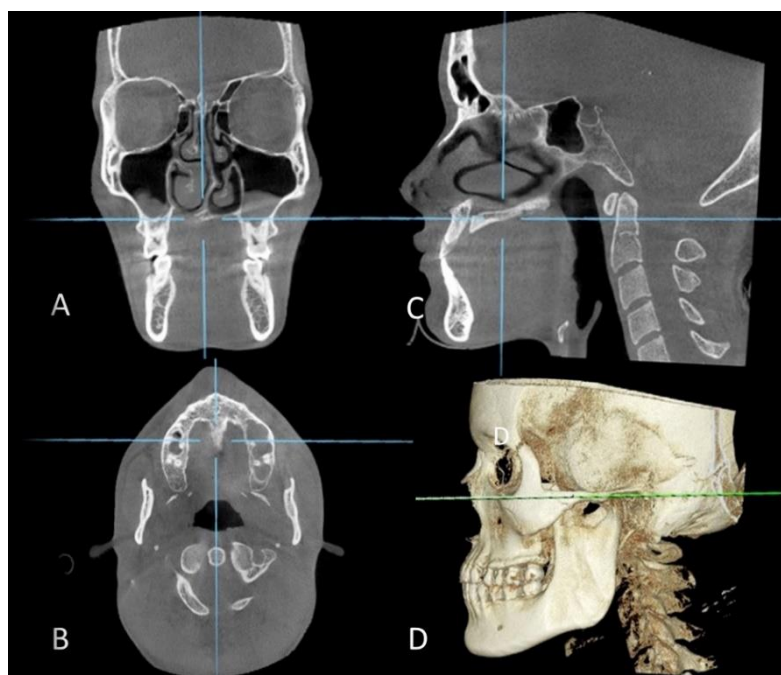
Ethical considerations

This cross-sectional study was approved by the Institutional Committee of Ethics with the register number 3.005.777. The CBCT images of 34 adults (14 men, 20 women), aged 18.0 to 57.7 years (mean age, 32.2 years) of mestizo ethnicity were selected from the database of a private tomographic laboratory in Santo Domingo, Dominican Republic, to assess the IZC crest region, according to the objectives mentioned. The CBCT images were acquired using a Promax 3D Max (Plan-meca Inc, Roselle, IL) device with an acquisition protocol of 90 kVp, 8–14 mA, 0.2mm-thick slices, 0.2-mm voxel size, and 20 × 20 cm field of view. The inclusion criteria were CBCT images of adult patients over 18.0 years old, no craniofacial anomalies, trauma or asymmetries, presence of complete maxillary and mandibular dentition with the exception of the third molars, no radiographic signs of bone resorption or periapical problems, and good image quality. All CBCT images that do not comply with the aforementioned inclusion criteria were excluded from this study.

Measurement protocol

Initially, each CBCT image was adjusted in order to set the head position, considering the sagittal slice perpendicular to the Frankfurt plane, the axial slice perpendicular to the midpalatal suture and the coronal slice perpendicular to the maxillary occlusal plane (plane formed between the distobuccal cusps of both maxillary first molars). All adjustments and measurements were performed using On Demand 3D software (On Demand 3D software version 1, Cyber Med, Seoul, South Korea) (Figure 1).

Figure 1. Tomographic adjustment: **A**, coronal slice; **B**, axial slice; **C**, sagittal slice; **D**, 3D reconstruction.



Source: Authors.

First, in the 3D reconstruction, the greatest prominence of the IZC region (GP-IZC) was determined in the frontal view and corroborated with the lateral view to determine the insertion site of the MI (Figure 2).

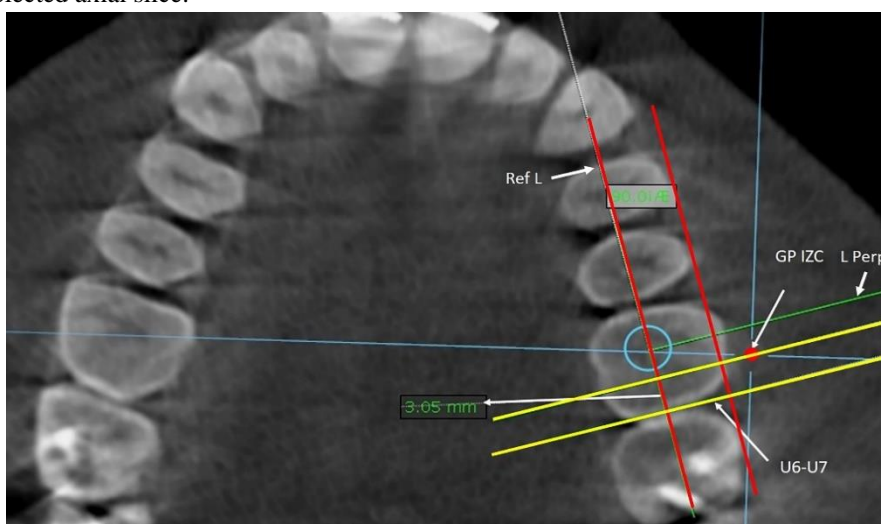
Figure 2. Determination of the greatest prominence of the Infrazygomatic crest region (red point) in 3D reconstruction for selection of the mini-implant insertion site: **A**, Frontal view; **B**, Lateral view.



Source: Authors.

The GP-IZC is comparatively the site chosen by digital palpation for MI insertion, when the clinician seeks for a site of greater prominence in the IZC region. Immediately, on the selected axial slice was evaluated its anteroposterior position relative to the dental reference located at the contact point of the crowns of the maxillary first and second molars (U6-U7) on each side. A reference line (Ref. L.) tangent to the vestibular surface of the premolars and molars was established. This line was moved to the center of the occlusal aspects of the crowns, and another line perpendicular (L. Perp.) to this reference line was constructed (Figure 3). Posteriorly, two lines parallel (yellow) to the L. Perp. were established, one passing through the selected GP-IZC (selected site for the MI insertion) and the other through the dental reference U6-U7. The distance between both lines provided the anteroposterior position of the greatest prominence of the IZC relative to the dental reference U6-U7 (Figure 3).

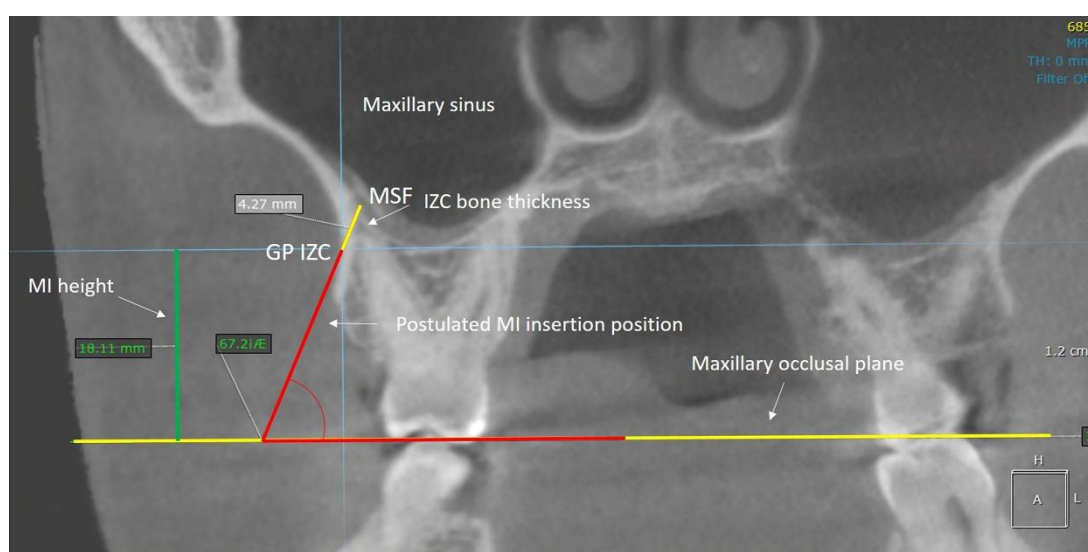
Figure 3. Evaluation of the anteroposterior position of the greatest prominence of the Infrazygomatic crest (mini-implant insertion site selected) relative to the dental reference located at the contact point of the crowns of U6-U7 on each side in the selected axial slice.



Source: Authors.

Second, on the selected coronal slice, two reference lines were established to evaluate the insertion angulation of the MI. The first reference line was the maxillary occlusal plane, a plane formed between the distobuccal cusps of both maxillary first molars. The second reference line was the postulated mini-implant insertion position, a line formed between the selected insertion site of the MI on the buccal cortical bone of the GP-IZC, until it made contact with the cortical bone of the maxillary sinus floor (MSF). The insertion angle of the MI was measured between the intersection of the postulated MI insertion position line and the maxillary occlusal plane. The IZC thickness was measured from GP-IZC to MSF. The same procedure was performed on slices at intervals of 1 mm for mesial and distal up to reach 4 mm, maintaining the same initial MI insertion height (Figure 4).

Figure 4. Coronal slice, reference lines constructed to measure the Infrazygomatic crest thickness and the mini-implant insertion angle and height.



Source: Authors.

Third, on the selected coronal slice, the height of the MI insertion point (greatest prominence of the IZC) was measured from the distobuccal cusp of the maxillary first molar to the GP-IZC.

All measurements were performed on the right and left sides.

Statistical analysis

A previously trained and calibrated investigator (O.M.A.R) performed all measurements on CBCTs under identical conditions. To test the reliability of the measurements, 30 CBCTs were randomly selected for re-measurement by simple random sampling 2 weeks after the initial measurement. The Dahlberg's error test was used to verify the reliability of the two-time measurements. All data collected were tabulated in an electronic database and later subjected to specific statistical analyses using the SPSS statistical program (version 25.0; IBM, Chicago, IL, USA).

Descriptive statistics were performed to identify the general and specific characteristics of the study sample. The normality assumptions were verified using the Kolmogorov-Smirnov test.

The paired Student's *t*-test was used to compare the measurements between the two sides and on the same side. Comparisons of measurements between sexes were performed using the Mann-Whitney U test. The level of significance used was $P < 0.05$.

3. Results

The Dahlberg's error test showed satisfactory reliability of the two-time measurements (< 20% error). The mean mesiodistal position of the GP-IZC was located 0.19 mm (± 1.79) mesial to U6-U7 on the right side and 0.29 mm (± 1.65) mesial to U6-U7 on the left side (Table 1).

The mean value of the greatest bone thickness of the IZC was 4.95 mm (± 2.39) on the right side and 4.79 mm (± 2.13) on the left side (Tables 2 and 3). There were no statistically significant differences when comparing the mean bone thickness values of the IZC region between genders.

The mean MI height above the maxillary occlusal plane was located 17.92 mm (± 2.23) on the right side and 17.58 mm (± 2.37) on the left side.

Table 1. Descriptive statistics of the mesiodistal position of the greatest prominence of the IZC assessed on both sides.						
					95% Confidence interval	
	Mean	Standard Deviation	Minimum	Maximum	Lower limit	Upper limit
Right side (mm)	0.19	1.79	-2.74	3.84	-0.43	0.81
Left side (mm)	0.29	1.66	-2.89	3.07	-0.28	0.86

Source: Authors.

Table 2. Descriptive statistics of IZC thickness evaluated in the coronal slice on the right side.						
					95% Confidence interval	
	Mean	Standard Deviation	Minimum	Maximum	Lower limit	Upper limit
4mm mesial	4.16	2.46	1.66	14.73	3.30	5.02
3mm mesial	4.09	2.42	1.69	13.90	3.25	4.94
2mm mesial	4.12	2.38	1.82	13.21	3.28	4.95
1mm mesial	4.13	2.32	1.72	12.24	3.31	4.94
Initial point	4.19	2.29	1.85	11.58	3.39	4.99
1mm distal	4.31	2.26	2.06	10.84	3.52	5.10
2mm distal	4.47	2.29	2.18	10.47	3.67	5.27
3mm distal	4.65	2.27	2.25	10.47	3.86	5.44
4mm distal	4.95	2.39	2.32	11.49	4.11	5.78

Source: Authors.

Table 3. Descriptive statistics of IZC thickness evaluated in the coronal slice on the left side

	Mean	Standard Deviation	Minimum	Maximum	95% Confidence	
					Lower limit	Upper limit
4mm mesial	4.60	2.51	1.73	13.24	3.73	5.48
3mm mesial	4.38	2.46	1.80	12.60	3.52	5.25
2mm mesial	4.32	2.34	1.75	11.64	3.50	5.14
1mm mesial	4.17	2.27	1.66	11.09	3.38	4.97
Initial point	4.11	2.13	1.67	10.61	3.36	4.85
1mm distal	4.17	2.09	1.57	11.03	3.44	4.90
2mm distal	4.27	2.04	1.84	11.35	3.56	4.98
3mm distal	4.53	2.04	1.93	11.72	3.82	5.25
4mm distal	4.79	2.13	2.08	12.25	4.05	5.54

Source: Authors.

Statistically significant differences found on comparing the mean bone thickness values between each slice studied on the same side are shown in Table 4 for the right side and in Table 5 for the left side. The bone tended to gradually become thicker distally in relation to the dental reference U6-U7 and the GP-IZC.

Table 4. Comparing the mean bone thickness between each slice on the right side.

	4mm mesial	3mm mesial	2mm mesial	1mm mesial	Initial point	1mm distal	2mm distal	3mm distal	4mm distal
4mm mesial									0.018
3mm mesial								0.037	0.005
2mm mesial								0.024	0.003
1mm mesial								0.016	0.002
Initial point							0.048	0.012	0.001
1mm distal								0.006	0.000
2mm distal								0.008	0.000
3mm distal									0.001

Source: Authors.

Table 5. Comparing the mean bone thickness between each slice studied on the left side

	4mm mesial	3mm mesial	2mm mesial	1mm mesial	Initial point	1mm distal	2mm distal	3mm distal	4mm distal
4mm mesial									
3mm mesial	0.001								
2mm mesial	0.029								
1mm mesial	0.014		0.032						0.031
Initial point	0.030							0.012	0.002
1mm distal								0.031	0.000
2mm distal								0.000	0.000
3mm distal									0.000
4mm distal									

Source: Authors.

	Right side	Standard deviation	Left side	Standard deviation	p value
Initial point	62.74	5.28	63.90	4.96	0.123
1 mm mesial	63.08	5.43	65.18	5.32	0.004
2 mm mesial	63.02	5.19	65.47	5.34	0.001
3 mm mesial	63.85	4.77	65.57	4.67	0.011
4 mm mesial	63.96	4.63	66.22	4.53	0.007
1 mm distal	63.40	5.34	64.96	5.86	0.013
2 mm distal	62.98	6.36	64.74	5.78	0.019
3 mm distal	62.75	6.15	65.03	4.79	0.014
4 mm distal	63.71	5.48	65.19	5.47	0.069

Source: Authors.

Comparing the right and left sides according to MI insertion angulation at each slice studied, statistically significant differences were found in most slices, except at point 0 ($P = 0.123$) and point 4 mm distally ($P = 0.069$) (Table 6). The mean value for MI insertion angulation on the right side was 63.28° and 65.14° on the left side.

There were no statistically significant differences when comparing the mean bone thickness values of the IZC region between the right and left sides ($P > 0.05$).

Between sexes, there were no statistically significant differences when comparing the mean bone thickness values in the 9 coronal slices studied in the IZC region ($P > 0.05$).

4. Discussion

Sometimes the clinician is based solely on his/her ability and clinical experience to insert MIs in the IZC region without CBCT of the area. For this reason, the clinical procedure performed by intraoral digital palpation of the GP-IZC for MI insertion in adults was simulated using CBCT.

In the present study, the mean position of the greatest prominence of the IZC was found to be 0.19 mm (± 1.79) mesial on the right side and 0.29 mm (± 1.65) mesial on the left side, relative to the dental reference U6-U7. This was determined visually in the 3D reconstruction of each patient, representing the clinical procedure by digital palpation performed by the clinician.

By the way, Liu et al (Liu et al., 2017) observed that the U6-U7 region is the most ideal safe zone for placing MIs in the buccal alveolar bone in the IZC region for maxillary dentition distalization.

The mean greatest bone thickness of the IZC was 4.95 mm (± 2.39) on the right side and 4.79 mm (± 2.13) on the left side, and it was located 3.81 mm distal to the dental reference U6-U7 on the right side and 3.71 mm distal on the left side. It was 17.92 mm (± 2.23) height above the maxillary occlusal plane on the right side and 17.58 mm (± 2.37) on the left side. The overall mean bone thickness was 4.35 mm. In relation to the mean IZC greatest prominence found, the IZC greatest thickness was located 4 mm distally on both sides. The bone tended to gradually become thicker distally in relation to the dental reference U6-U7 and the GP-IZC.

Some studies have evaluated the IZC in terms of bone thickness, MI insertion angle, and height using CBCT. In 2007, Liou et al (Liou et al., 2007) measured the thickness of the IZC above the mesiobuccal root of the maxillary first molars at different angles and positions and recommended 6 mm as the minimal IZC thickness for sustaining an MI, inserting it 14 to 16 mm height at an angle of 55° to 70° to the maxillary occlusal plane. Baumgaertel et al (Baumgaertel & Hans, 2009) investigated the thickness of the IZC at three sites above the maxillary first molar and found an average bone depth of 6.17 to 7.05 mm at the

lowest measurement level selected; thereafter, the values gradually decreased until reaching the most apical measurement of 2.97 to 3.6 mm. Placement at the first level would violate the minimal safety recommended distance for MIs insertion. In addition, Santos et al (Santos et al., 2017) evaluated the IZC at two selected points above the distobuccal root of the maxillary first molars and found an overall mean IZC thickness of 2.49 mm and 2.29 mm, respectively.

In the present study, the average bone thickness of IZC was lower than the values obtained by Liou and Baumgaertel. (Baumgaertel & Hans, 2009; Liou et al., 2007) This was probably owing to the following circumstances. First, a certain safety distance is required. Maino et al (Maino et al., 2005) recommended 0.5 mm as the minimal safety distance to any adjacent anatomical structure, and Baumgaertel (Baumgaertel & Hans, 2009) also used 0.5 mm; nevertheless, Liou et al (Liou et al., 2004) recommended 2 mm. In our study, 1.25 mm was the minimal safety distance used. Therefore, it was necessary to place the MIs in a more apical position, which resulted in a concomitant reduction of the IZC bone thickness. Second, the amount of alveolar process height and depth; the buccal bone available surrounding the posterior maxillary roots in several patients was very thin to support an MI; therefore, it was necessary to insert the MIs in a more apical position, resulting in a reduction of the IZC thickness. Third, maxillary sinus pneumatization size; roots of the maxillary posterior teeth frequently cause convolutions in the floor of the sinus, resulting in a reduction of the IZC thickness. Fourth, root length and buccolingual inclination of the maxillary first and second molars; the greater the root length and buccal root inclination, the lesser the thickness of the IZC.

In contrast, the values obtained by Santos et al (Santos et al., 2017) were significantly lower than those obtained in the present study because the MI insertion site selected by them was even more apical. In summary, the more apical the selected MI insertion site, the lesser the bone thickness.

As mentioned above, Liou (Liou et al., 2007) recommended 6 mm as the minimal IZC thickness for sustaining a MI, nevertheless, Costa et al (Costa et al., 1998) and Miyawaki et al (Miyawaki et al., 2003) mentioned that the cortical bone quality and quantity are the major factors associated with primary stability. Farnsworth et al (Farnsworth et al., 2011) reported that the average cortical thickness of the IZC is only 1.44 to 1.58 mm. As generally accepted, cortical bone thickness of more than 1 mm is required for good stability of orthodontic MI. The thickness of the buccal cortical bone was not directly evaluated in the present study, but the total thickness of the IZC according to the MI insertion angle was measured from the buccal cortical bone to the cortical bone of the MSF. In this way, the MI insertion reaches bicortical fixation, achieving adequate primary stability by mechanical retention.

Among the risks mentioned during the insertion of MIs in the IZC is also the possibility of penetrating and damaging the maxillary sinus. Jia et al (Jia et al., 2018) determined the incidence of IZC MIs penetration into the maxillary sinus in clinical practice using CBCT. The overall success rate of MIs inserted in the IZC was 96.7%, and 78.3% penetrated into the maxillary sinus. They concluded that the incidence of penetration of IZC MIs into the sinus may be high, and penetration through double cortical bone plates with limitation of penetration depth within 1 mm is recommended. On the other hand, Chang et al (Chang et al., 2022) evaluated the success rate of MIs placed in the Infrazygomatic crest in relation to maxillary sinus penetration. They observed that 48% of MI penetrated the maxillary sinus with a mean penetration length of 3.23 mm, however they concluded that maxillary sinus perforation has no significant effect on MI survival, and none patient reported any adverse signs or symptoms of sinus perforation. In the present study, the importance of bicortical penetration of MIs in the IZC to obtain adequate primary stability was considered.

Lee et al (Lee et al., 2013) found that the IZC was clinically thicker in males than in females. In contrast, Santos et al (Santos et al., 2017) mentioned that no statistically significant differences were detected between gender. In the present study, there were no statistically significant differences when comparing the mean bone thickness values of the IZC region between sexes.

In concordance with Lee et al (Lee et al., 2013), we found no statistically significant differences when comparing the

mean bone thickness values of the IZC region between the right and left sides. Comparing the right and left sides according to MI insertion angulation at each slice studied, differences were found in most slices, except at point 0 and point 4 mm distally. The average insertion angle of MI on the left side was higher compared to the right side.

A limitation of this study was that individuals in the sample were from a specific country with possible ethnic skeletal features; therefore, caution is recommended when extrapolating these results to other populations. Nevertheless, the results presented can be used as clinical knowledge to guide procedures of MI insertion in the IZC region.

As a suggestion to conduct a future study, it is recommended to have a larger sample size to clarify the findings presented in this research.

5. Conclusion

Sometimes the operator is based solely on his/her ability and clinical experience to insert MIs in the IZC without aid of CBCT. For this reason, the clinical procedure performed by intraoral digital palpation of the GP-IZC for MI insertion in adults was simulated using CBCT, to have predictable clinical reference in the insertion of MIs.

The GP-IZC determined visually on the 3D reconstruction, did not present the greatest bone thickness. The bone tended to gradually become thicker distal to the GP-IZC (MI insertion site selected by the operator) and the dental reference U6-U7.

Acknowledgments

The authors thank Dr Alexis Ovalle and Eng Francisco Ovalle for the help in the acquisition of the CBCT images, and Dr Caio Manfro Bianeck, radiologist imaginologist for the help in the CBCT measurements.

References

- Ali, D., Mohammed, H., Koo, S.-H., Kang, K.-H., & Kim, S.-C. (2016). Three-dimensional evaluation of tooth movement in Class II malocclusions treated without extraction by orthodontic mini-implant anchorage. *Korean J Orthod*, *46*(5), 280-289. 10.4041/kjod.2016.46.5.280
- Baumgaertel, S., & Hans, M. G. (2009). Assessment of infrazygomatic bone depth for mini-screw insertion. *Clin. Oral Implants Res*, *20*(6), 638-642. 10.1111/j.1600-0501.2008.01691.x
- Chang, C. H., Lin, J.-H., & Roberts, W. E. (2022). Success of infrazygomatic crest bone screws: patient age, insertion angle, sinus penetration, and terminal insertion torque. *Am J Orthod Dentofacial Orthop*. 10.1016/j.ajodo.2021.01.028
- Chang, C. H., Lin, J. S., & Roberts, W. E. (2019). Failure rates for stainless steel versus titanium alloy infrazygomatic crest bone screws: A single-center, randomized double-blind clinical trial. *Angle Orthod*, *89*(1), 40-46. 10.2319/012518-70.1
- Costa, A., Raffainl, M., & Melsen, B. (1998). Miniscrews as orthodontic anchorage: a preliminary report. *Int J Adult Orthodon Orthognath Surg*, *13*(3), 201-209.
- De Clerck, H., Geerinckx, V., & Siciliano, S. (2002). The zygoma anchorage system. *J Clin Orthod*, *36*(8), 455-459.
- Farnsworth, D., Rossouw, P. E., Ceen, R. F., & Buschang, P. H. (2011). Cortical bone thickness at common miniscrew implant placement sites. *Am J Orthod Dentofacial Orthop*, *139*(4), 495-503. 10.1016/j.ajodo.2009.03.057
- Jia, X., Chen, X., & Huang, X. (2018). Influence of orthodontic mini-implant penetration of the maxillary sinus in the infrazygomatic crest region. *Am J Orthod Dentofacial Orthop*, *153*(5), 656-661. 10.1016/j.ajodo.2017.08.021
- Keles, A., & Sayinsu, K. (2000). A new approach in maxillary molar distalization: intraoral bodily molar distalizer. *Am J Orthod Dentofacial Orthop*, *117*(1), 39-48. 10.1016/s0889-5406(00)70246-0
- Lee, H.-S., Choi, H.-M., Choi, D.-S., Jang, I., & Cha, B.-K. (2013). Bone thickness of the infrazygomatic crest area in skeletal Class III growing patients: A computed tomographic study. *Imaging Sci Dent*, *43*(4), 261-266. 10.5624/isd.2013.43.4.261
- Lima Jr, A., Domingos, R. G., Ribeiro, A. N. C., Neto, J. R., & de Paiva, J. B. (2022). Safe sites for orthodontic miniscrew insertion in the infrazygomatic crest area in different facial types: A tomographic study. *Am J Orthod Dentofacial Orthop*, *161*(1), 37-45. 10.1016/j.ajodo.2020.06.044

- Liou, E. J., Chen, P.-H., Wang, Y.-C., & Lin, J. C.-Y. (2007). A computed tomographic image study on the thickness of the infrazygomatic crest of the maxilla and its clinical implications for miniscrew insertion. *Am J Orthod Dentofacial Orthop*, *131*(3), 352-356. 10.1016/j.ajodo.2005.04.044
- Liou, E. J., Pai, B. C., & Lin, J. C. (2004). Do miniscrews remain stationary under orthodontic forces? *Am J Orthod Dentofacial Orthop*, *126*(1), 42-47. 10.1016/j.ajodo.2003.06.018
- Liu, H., Wu, X., Yang, L., & Ding, Y. (2017). Safe zones for miniscrews in maxillary dentition distalization assessed with cone-beam computed tomography. *Am J Orthod Dentofacial Orthop*, *151*(3), 500-506. 10.1016/j.ajodo.2016.07.021
- Maino, B. G., Bednar, J., Pagin, P., & Mura, P. (2003). *Miniscrew implants: the spider screw anchorage system*. *37*(2), *J Clin Orthod*, 90-97.
- Miyawaki, S., Koyama, I., Inoue, M., Mishima, K., Sugahara, T., & Takano-Yamamoto, T. (2003). Factors associated with the stability of titanium screws placed in the posterior region for orthodontic anchorage. *Am J Orthod Dentofacial Orthop*, *124*(4), 373-378. 10.1016/s0889-5406(03)00565-1
- Murugesan, A., & Sivakumar, A. (2020). Comparison of bone thickness in infrazygomatic crest area at various miniscrew insertion angles in Dravidian population—A cone beam computed tomography study. *Int Orthod*, *18*(1), 105-114. 10.1016/j.ortho.2019.12.001
- Santos, A. R., Castellucci, M., Crusoé-Rebello, I. M., & Sobral, M. C. (2017). Assessing bone thickness in the infrazygomatic crest area aiming the orthodontic miniplates positioning: a tomographic study. *Dental Press Journal of Orthodontics*, *22*, 70-76.
- Uribe, F., Mehr, R., Mathur, A., Janakiraman, N., & Allareddy, V. (2015). Failure rates of mini-implants placed in the infrazygomatic region. *Prog Orthod*, *16*(1), 1-6. 10.1186/s40510-015-0100-2
- Vargas, E. O. A., de Lima, R. L., & Nojima, L. I. (2020). Mandibular buccal shelf and infrazygomatic crest thicknesses in patients with different vertical facial heights. *Am J Orthod Dentofacial Orthop*, *158*(3), 349-356. 10.1016/j.ajodo.2019.08.016
- Wu, J.-H., Lu, P.-C., Lee, K.-T., Du, J.-K., Wang, H.-C., & Chen, C.-M. (2011). Horizontal and vertical resistance strength of infrazygomatic mini-implants. *Int J Oral Maxillofac Surg*, *40*(5), 521-525. 10.1016/j.ijom.2011.01.002